PHASE MODULATION WITH INDEPENDENT CAVITY-PHASE CONTROL IN LASER COOLED CLOCKS IN SPACE*

W.M. Klipstein†, G.J. Dick†, S.R. Jefferts‡, F.L. Walls‡

†California Institute of Technology
Jet Propulsion Laboratory
Pasadena, California

‡National Institute of Standards and Technology
Boulder, Colorado

Abstract

The standard interrogation technique in atomic beam clocks is square-wave frequency modulation(SWFM), which suffers a first-order sensitivity to vibrations as changes in the transit time of the atoms translates to perceived frequency errors. Square-wave phase modulation (SWPM) interrogation eliminates sensitivity to this noise. We present a particular scheme utilizing independent phase control of the two cavities. The technique is being considered for use with the Primary Atomic Reference Clock in Space (PARCS), a laser-cooled cesium clock scheduled to fly aboard the International Space Station in 2005. In addition to eliminating first-order sensitivity to vibrations, the minimum attack time now in this scheme is the Rabi pulse time (t), rather than the Ramsey time (T). This helps minimize dead time and the degradation of stability due to aliasing.

1 Introduction

The vibration spectrum on the International Space Station (ISS) is expected to be sufficiently severe that it can cause serious problems for atomic clocks using laser-cooled atoms and traditional (SWFM) techniques. As a result, we propose as a solution for the PARCS[1] clock, an old idea, dating back to Ramsey[2], of using phase modulation. SWPM is relatively easily realized in many modern frequency synthesizers which depend on direct digital synthesizers(DDS)[3, 4] as a part of the synthesis chain. SWPM has several distinct advantages over SWFM, most importantly for PARCS, the vibration sensitivity is reduced by orders of magnitude. The actual implementation of SWPM for PARCS will use two independent frequency synthesizers, one driving each of the Ramsey interaction zones. With this topology, the duty cycle of the clock is significantly enhanced for the case of multiple launches per "lineside" (or phase). Lastly, a whole class of systematic frequency shifts is greatly suppressed as will be discussed in a later paper[5].

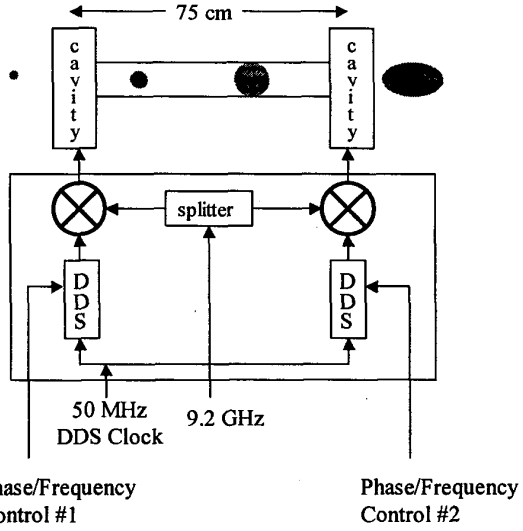

Figure 1: The PARCS Ramsey zone (shown schematically) with independent phase control of the two cavities.

While the focus of the present paper is towards laser-cooled atomic clocks in space, with two separated Ramsey interaction zones, many of the advantages apply equally well to other clock geometries, including traditional thermal beam clocks, pulsed fountain clocks and continuous fountain clocks[6]. We have tested SWPM in October 1999 on NIST-F1, the NIST primary frequency standard (a pulsed cesium fountain) and found no significant frequency offset relative to SWFM at the 10^{-15} level. SWPM has also recently been implemented on the USNO cesium fountain with success[7].

*Part of the research described in this paper is work of the US Government, not subject to US copyright. Part of the research described in this paper was carried out at the Jet Propulsion Laboratory, California Institute of Technology, under a contract with the National Aeronautics and Space Administration.

0-7803-7028-7/01/$10.00 © 2001 IEEE

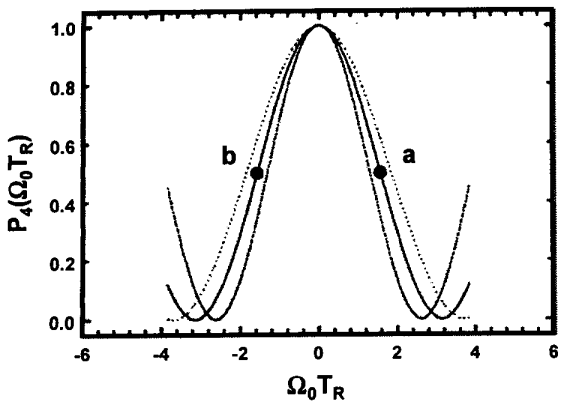

Figure 2: The central Ramsey fringe with no vibration is shown solid while the effects of vibration are shown as dotted fringes. The points **a** and **b** are the FWHM of the fringe, which is the normal modulation using SWFM.

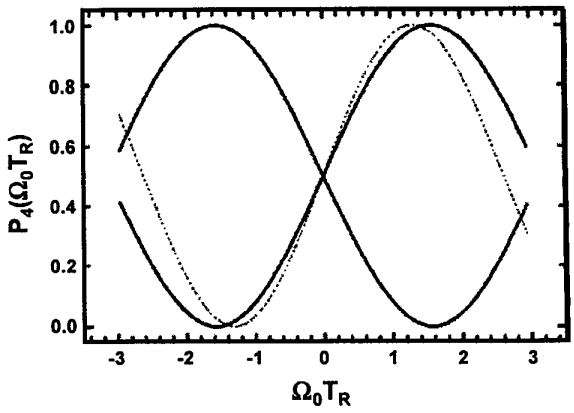

Figure 3: The central Ramsey fringe under $\pi/2$ phase modulation conditions. The servo steers the frequency to the fringe crossing point. The effect of vibration is illustrated by the dotted fringe.

2 Line Shape and Modulation

PARCS, as shown schematically in Figure 1, has two Ramsey interaction zones separated by 75 cm. In the vicinity of the central Ramsey fringe the fringe can be described by

$$P_4 = \frac{1}{2}\left[1 + \cos\left(\Omega_0 T_\tau + \phi\right)\right] \sin^2\left(b\tau\right) \qquad (1)$$

where P_4 is the probability of transition from the $|3,0>$ to the $|4,0>$ level, Ω_0 is the offset from the resonance frequency, $\Omega = \omega - \omega_0$, T_R is the Ramsey time, and ϕ is the phase angle between the microwave fields in the two Ramsey interaction zones[8].

In the usual Ramsey interrogation technique, ϕ is set equal to zero and the interrogation frequency is modulated between the points a and b in Figure 2. The frequency at point a (or b) is adjusted to be higher (lower) by an amount $\delta\omega$ such that the phase of the microwave field in the second Ramsey interaction leads (lags) the phase of the atomic superposition by $\pi/2$ at a given Ramsey time of T_R. If P_4(a) is larger (smaller) than P_4(b), the synthesizer frequency is lowered (raised) by an appropriate amount so that P_4(a)=P_4(b). The relative phase between the atomic superposition and the microwave field in the second Ramsey zone therefore depends on the Ramsey time. Vibrations of the atomic clock along the atomic trajectory will change the Ramsey time resulting in Ramsey resonances depicted by the dotted lines in Figure 2. These vibrations cause noise in the clock as a result of this "breathing" of the width of the Ramsey fringe[9].

If ϕ in equation(1) is set to $\pi/2$ instead of 0 then the resulting Ramsey curve has either a rising or falling dispersion shape as shown in Figure 3. The $\pi/2$ phase difference between the two Ramsey interactions causes the P_4(a)=P_4(b) point to occur at the resonance frequency of the atom. The frequency servo now works by first measuring P_4 for $+\pi/2$ relative phase between the Ramsey zones and then $-\pi/2$. The frequency is adjusted so that $P_4(\pi/2) = P_4(-\pi/2)$. Because the phase of the microwave field is advancing at the same rate as the phase of the atomic superposition, changes in the Ramsey time do not affect the relative phase between the atomic superposition and the microwave field in the second Ramsey interaction zone. Changes in the Ramsey time cause the slope of the dispersion curve to change, as is illustrated by the dotted lines in Figure 3, but the crossing point (i.e. the point $P_4(\pi/2) = P_4(-\pi/2)$) is unchanged. This insensitivity to Ramsey time greatly reduces the vibration sensitivity of the atomic clock as will be shown below.

An additional advantage of the independent phase modulation technique is realized in the PARCS clock which launches many (of order 10) balls of atoms at either $\pi/2$ of phase lag or lead. In a traditional SWFM modulation scheme the servo must be blanked for a time on the order of the transit time of the atoms through the clock $\approx T_R$ between frequencies above and below the resonance. This blanking time contributes to the dead time and therefore increases aliasing of the local oscillator noise (Dick Effect)[10]. When using SWPM, however, the servo blanking time is reduced to the atom transit time through the second Ramsey cavity- and the dead time fraction therefore reduced, thus reducing the aliasing effect. The reduction in dead time fraction also reduces the total number of atoms which must be launched in order to support a given short term frequency stability, thus reducing the magnitude of the spin exchange frequency shift as well as relaxing the short term stability requirements on the local oscillator through the aforementioned reduction in aliasing.

This technique (SWPM) has significant terrestrial applications as well[11].

3 Impact of Random Accelerations on Frequency Stability

Interrogation errors due to unwanted accelerations of the waveguide structures used to distribute microwave signals to two physically separated interrogation sites can substantially degrade the performance of a laser-cooled frequency standard. In such a standard, slow-moving lasercooled bunches of atoms are sequentially interrogated as they arrive at one and then the other of the two interrogation regions. Errors arise if the phase of the microwave signal is systematically varied with respect to the atomic phase itself.

3.1 FM Effects

As discussed in the previous section, an error arises with frequency modulation interrogation when physical acceleration of the beam tube causes microwave interrogations to take place too soon or too late, giving rise to an unwanted phase difference between atoms and L.O. due to the FM frequency offset.

The effect of random motions of the beam tube $x(t)$ have been previously analyzed in terms of an aliasing effect, where motions at frequencies near $f = 1/2T_c$ are aliased to near zero frequency[9]. Using an approach similar to that developed in Ref. [9], we first calculate a fractional frequency variation $y(f)$ due to sinusoidal motion components $x(f)$ along the axis of the drift space for any frequency f as:

$$y_{fm}(f) = \frac{x(f)}{4t_i\nu_0 L}, \tag{2}$$

where t_i is the interrogation (drift) time, and where we assume the usual $\pi/2$ phase progression during the interrogation.

Because the characteristics of the ISS are given in terms of accelerations as $S_a(f)$ we rewrite the previous equation in terms of spectral densities as:

$$S_y^{fm} = \frac{S_a(f)}{(2\pi f)^4}\frac{1}{(4t_i\nu_0 L)^2}. \tag{3}$$

However, the frequency error induced by a motion-delayed measurement of any atom shows periodic sign reversals due to the frequency modulation interrogation process, and so slow variations will show an aliasing effect, with the lowest frequencies effectively eliminated, while other higher frequencies are aliased to near zero frequency. Actual aliasing amplitudes will depend on details of the interrogation strategy; dead time, etc.

We now calculate the effect for a model of SWFM with no dead time. This model gives aliased responses at odd harmonics of the modulation frequency, with amplitudes given by the harmonic content of a square wave with unit amplitude.

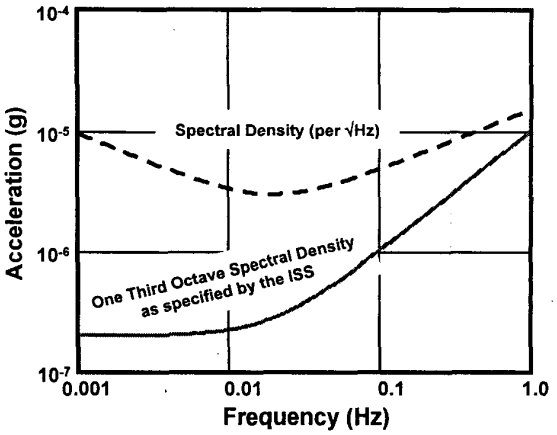

Figure 4: Smoothed approximation to ISS vibration specification. Shown are both the 1/3 octave form as specified by the ISS and the more traditional $Hz^{-1/2}$ form used in our calculations.

Thus, when the frequency standard is interrogated with a half-cycle (frequency measurement) time of T_c, its operation will show aliased frequency fluctuations $S_y^a(0)$ as:

$$S_y^a(0) = \left(\frac{2}{\pi}\right)^2 \sum_{n=1,3,..}^{\infty} \left[S_y^{fm}\left(\frac{n}{2t_c}\right)\frac{1}{n^2}\right]. \tag{4}$$

This spectral density gives rise to an Allan deviation limit to the performance of the frequency standard of

$$\sigma_y^a(t) = \sqrt{\frac{CS_y^a(0)}{\tau}}, \tag{5}$$

where C=1/2.

Figure 4 shows a smoothed plot of the acceleration spectrum expected on the ISS together with a conversion from the 1/3 octave plot to a more conventional spectral density of acceleration. Together with equations (4) and (5), this allows us to calculate an expected limitation to the performance. The result of this calculation is shown in Figure 5.

It is clear from Figure 5 that any problems due to FM interrogation are strongly dependent on the operating conditions of the frequency standard. For a short interrogation and a half cycle time of 1 second, as is planned for PHARAO, the aliasing effect is small. PARCS is expected to operate with multiple balls of atoms per "lineside", long Ramsey times, a high-performance hydrogen maser local oscillator(LO) and half cycle times of typically 50 s, a process that involves hundreds of balls of atoms. For this case, aliased noise is clearly an issue because the performance is marginal compared to the PARCS design stability of $5 \times 10^{-14}/\sqrt{\tau}$. Also, PARCS

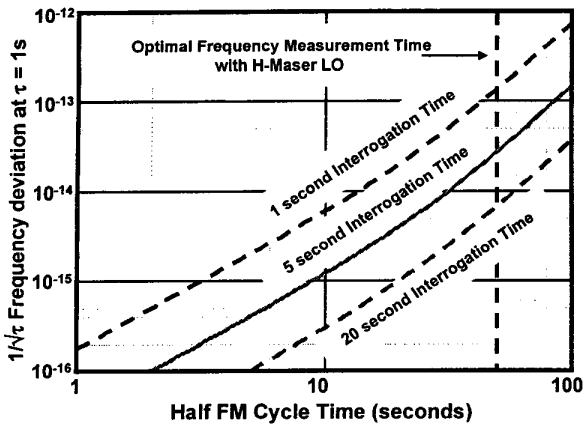

Figure 5: Vibration-induced limitation to white frequency noise performance due to aliasing with FM interrogation. Nominal PARCS conditions are a 5 second interrogation (drift) time and a 50 second frequency measurement time to match performance of the H-maser L.O.

is expected to operate before ISS construction is complete, during which time microgravity conditions are not obtained and under these conditions frequency stability would be substantially degraded.

3.2 Other Effects

The linear phase progression as the atoms drift down the beam tube can be eliminated by the use of interrogation schemes using SWPM instead of frequency modulation. This eliminates the large frequency sensitivity discussed above.

However, there remain several smaller effects which are discussed here. It is worth mentioning that the signs of these remaining smaller effects do not reverse during the course of either phase or frequency modulation, and so the sensitivity to very low frequency physical acceleration is not reduced by averaging over many interrogation cycles.

3.3 Phase Delay

Even if the microwave interrogation structures move rigidly, any motion will give rise to phase shifts between the two interrogating cavities due to the fact that the microwave photons are not dragged with the waveguide structure that feeds the interrogating microwave signals to the cavities. Here we assume that the waveguides are empty and not filled with a dielectric. For this effect we write:

$$\begin{aligned} y_{pd}(f) &= \frac{\delta\phi(f)}{\phi} = \frac{\frac{\dot{x}(f)}{c}\frac{L}{\lambda=c/\nu_0}}{\nu_0 t_i} \\ &= \dot{x}(f)\frac{L}{c^2 t_i} = x(f)\frac{2\pi f L}{c^2 t_i}. \end{aligned} \tag{6}$$

3.4 Mechanical Compression

A phase error can also result from mechanical compression of the waveguide structure under acceleration. Linear compression under a uniform acceleration $a(f)$ where $f \approx 0$ is given by:

$$\begin{aligned} \delta L(f) &= a(f)\frac{\rho L^2}{2Y} = a(f)\frac{L^2}{2v_s^2} \\ &= (2\pi)^2 f^2 \delta x(f)\frac{L^2}{2v_s^2}, \end{aligned} \tag{7}$$

where ρ is the material density and Y is the stiffness which combine to give the speed of sound as $v_s = \sqrt{Y/\rho}$. A change in waveguide length changes the rf phase to give rise to an imputed frequency error as:

$$y_{mc}(f) = \frac{\delta\phi(f)}{\phi} = \frac{\delta L(f)/\lambda}{\nu_0 t_i} = \frac{\delta L(f)}{c t_i}, \tag{8}$$

and so

$$\frac{y_{mc}(f)}{\delta x(f)} = \frac{2\pi^2 f^2 L^2}{v_s^2 c t_i}. \tag{9}$$

3.5 Total PM Sensitivity

Combining equations (6) and (9), we obtain for the total PM sensitivity:

$$\frac{y_{pm}(f)}{\delta x(f)} = \frac{2\pi f L}{c^2 t_i}\left(1 + \frac{\pi c L f}{v_s^2}\right). \tag{10}$$

3.6 Comparison

We can compare the phase delay and mechanical-compression frequency tunings with that due to FM interrogation, irrespective of aliasing, and a comparison that is valid at frequencies higher than $f = 1/(2t_c)$. Plugging in values of $\nu_0 = 10^{10}$, $v_s = 10^4$ m/s, $L = 1$ m, and $t_i = 10$ seconds into Eq. (2) gives a frequency sensitivity of

$$\frac{y_{fm}(f)}{a(f)} \approx 2.5 \times 10^{-12}\left(\frac{1\text{Hz}}{f}\right)^2 /g \tag{11}$$

for FM, while the underlying electromagnetic and electromechanical effects described by Eq. (10) combine to give a motion sensitivity for SWPM of

$$\frac{y_{pm}(f)}{a(f)} \approx 2.5 \times 10^{-18}\left(1 + \frac{0.1\text{Hz}}{f}\right) /g, \tag{12}$$

values that are some 6 orders of magnitude lower than the (additional) sensitivity effect for the FM case given by Eq. (11).

Note that while the FM term is a true position dependence, the two terms in the PM expression are actually velocity and acceleration dependencies, respectively. Thus while the PM terms do not show the nominally zero sensitivity at the lowest frequencies that characterize FM modulation, the terms are smaller by a power of f or f^2 at these low frequencies.

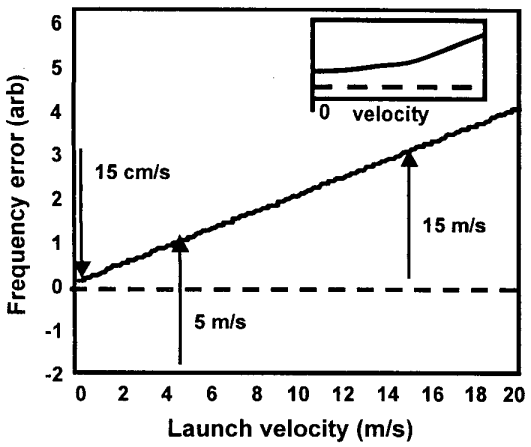

Figure 6: The apparent frequency error due to a phase offset between the cavities is linearly proportional to atomic velocity. By comparing the clock frequency for launch velocities of 5 and 15 m/s we can evaluate the end-to-end phase error, which can be removed with the independent phase control. Normal clock operation involves a launch velocity of 15 cm/s. The inset (not to scale) shows that for slow launches other effects cause the clock to deviate from the simple straight line.

4 Independent Phase Control

The main operational difficulty in implementing independent phase control of the two cavities is in evaluating and maintaining the end-to-end cavity phase shift. In traditional beam tubes this shift results from differing electrical path lengths to the two cavities, a quantity which is typically extremely stable as it results from the mechanical properties of the waveguide only. This typically is evaluated by reversing the direction of the beam through the cavities and comparing the results.

In the cesium instrument of PARCS beam reversal is not practical, but several additional handles are available. Specifically, laser cooling provides extremely narrow velocity distributions, the ability to vary the launch velocity, over two orders of magnitude, and constant velocities after launch, in the absence of gravity. Since the end-to-end shift is truly a phase offset, the apparent frequency error of interest can be related to the phase offset from Eqn.(1) as:

$$\delta\Omega_{end} = \frac{\phi_{end}}{T_R}. \tag{13}$$

For separation, L, between the two microwave cavities, the frequency error can be expressed in terms of the launch velocity as

$$\delta\Omega_{end} = \frac{\phi_{end}\nu_{launch}}{L}. \tag{14}$$

Eqn. (14) makes explicit the utility of varying the launch velocity as a technique for extracting the phase error,

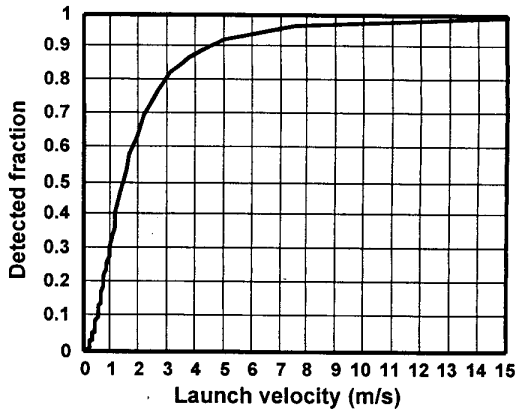

Figure 7: Fraction of atoms detected as a function of launch velocity.

ϕ_{end}. Measuring the clock frequency over a range of velocities allows a determination of the phase-offset as shown in Figure 6. The phase error could then be corrected by the synthesizer controlling the second cavity.

The performance goals of PARCS include accuracy of 5×10^{-17}, which for a 5 s Ramsey time means that phase offsets must be known to 14 μrad. Just as long Ramsey times mitigate the effect of phase errors on the fractional frequency performance of the clock, so too can higher launch velocities make the phase errors measurable. Launch velocities of 10s of meters per second are attainable, with 15 m/s representing a 100-fold increase over the standard operation of PARCS, using 15 cm/s launches. Varying the launch velocity obviously impacts more than just the end-to-end shift, requiring some care in order to separate out the piece linear in velocity. First, one might worry that operating at high velocities would compromise the stability of the clock, since the line Q degrades linearly with velocity. However, since most launched atoms are never detected due to thermal expansion of the cloud, the immediate result of increasing the launch velocity is to increase the number of detected atoms getting through the final aperture, roughly

$$N_{det} \propto \nu_{launch}^2. \tag{15}$$

Figure 7 shows the detected fraction of atoms under some simplifying assumptions about the operating conditions of PARCS.

The net result of increasing the launch velocity is that the stability improves as

$$\sigma_y(\tau) \propto \sqrt{\nu_{launch}}. \tag{16}$$

This improvement holds up to the point at which most launched atoms are detected, which occurs at roughly 2 m/s, above which the stability would begin to degrade due to the diminishing line Q.

Variation of the clock stability as a function of launch velocity is shown in Figure 8. This comparison assumes

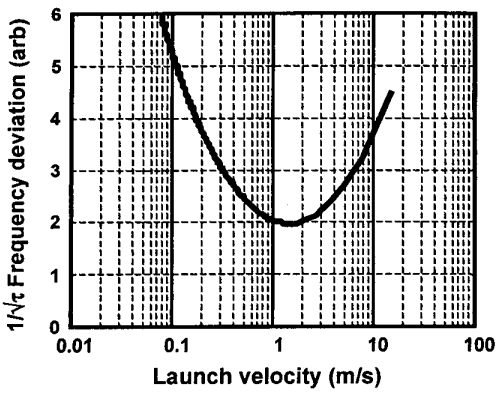

Figure 8: Relative clock stability as a function of launch velocity. The stability improves for faster launches as the detected fraction increases. Once most atoms are detected the loss in line Q reduces the stability.

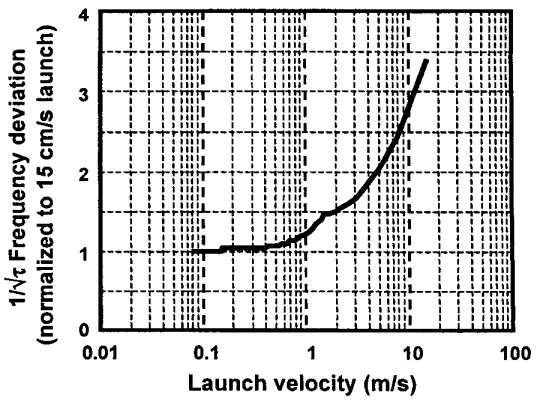

Figure 9: Relative clock stability for PARCS using multiple balls, showing a recovery of stability for slow launches. Stability has been normalized to normal clock operation at 15 cm/s. Shutters in the atomic beam path prevent light shifts.

no dead time and only one ball launched at a time, illustrating the trade-off between detected atom fraction and line Q. PARCS plans to use shutters in the atom beam to allow multiple balls to be collected and launched within a single Ramsey time without suffering from light shifts, which allows us to reclaim some of our lost stability as shown in Figure 9.

The stability calculated in Figure 9 assumes that the load time has been fixed (at 0.25 seconds) to keep the conditions of atom collection constant. This condition can be met provided the Ramsey time is at least as long as the load time. For launch velocities faster than 3 m/s, the load time determines the cycle time, and there is an additional duty cycle factor as shown in Figure 10. Including this factor, the net stability under the chosen operating conditions are shown in Figure 11.

As previously indicated, PARCS has a design stability of $5 \times 10^{-14}/\sqrt{\tau}$, and a design accuracy goal of 5×10^{-17}. If we allocate 2×10^{-17} from our error budget to the end-to-end uncertainty, we can now evaluate how long we must average to realize our design goals. For the purpose of illustration, consider at what τ we will have averaged down to a deviation of 10^{-15} for launches of 5 and 15 m/s: 17,000 seconds and 143,000 seconds respectively. If we define $f(v)$ as the measured clock frequency for atoms launched at v m/s, then we can write the difference between the average frequencies at these two launch velocities as

$$\begin{aligned} f(15) - f(5) &= (f_0 + 100\Delta) - (f_0 + 33\Delta) \\ &= 67\Delta, \end{aligned} \tag{17}$$

where Δ is the frequency error due to residual end-to-end phase shift for a launch velocity of 15 cm/s, and f_0 is an operational frequency that includes all other effects at these two launch velocities. f_0 should not be confused with $f(0.15)$, the frequency of the clock in normal operation. The uncertainty in this frequency difference is 1.4×10^{-15}, giving a fractional frequency uncertainty in Δ of 2×10^{-17}. The τ at which the clock realizes its accuracy floor is 10^6 seconds, so to meet our goals we must average 16% of the time, assuming we need to do the evaluation on an ongoing basis.

This example is clearly not the optimized solution for averaging time, but has been presented for its simplicity. There are several avenues for reducing the fractional time by a factor of three or so, but this sets the scale and makes the trade-offs and limitations clear.

The final question in our example is whether f_0 from Equation 17 is a constant in comparing the frequencies associated with these two launch velocities. That is, will $f(5m/s)$ differ from $f(15m/s)$ only due to the phase offset between the two cavities. Of the dominant offsets in the clock, the one which seems most worrisome is the cold-atom collisional shift, which is made up of two parts. The first is the density dependence, and the second is the interatomic collisional energy. These frequency offsets must be constant within the 10^{-15} level of the comparison, but need not be known absolutely. For the two fast launch velocities, the density only varies by 3%, so the shift must be below 3×10^{-14}, a condition which is easily satisfied. Of equal importance to the density is the collision energy involved in interatomic collisions, as the frequency shift is a strong function of energy as calculated by Williams and co-workers at NIST (submitted to Phys. Rev. A, 2000), growing in magnitude and even changing sign. Just after launch, the collision energy is roughly the thermal energy until the cloud has expanded an amount comparable to its initial size. Then the collision energy is dominated by phase space considerations: atoms at the same point in space must

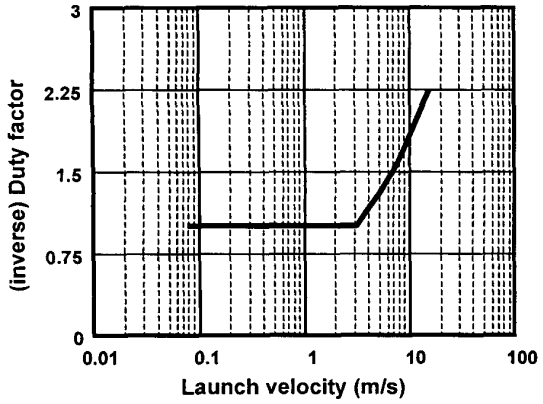

Figure 10: Clock stability is further degraded at high velocities by a reduced duty factor when the Ramsey time is less than the load time (0.25 seconds).

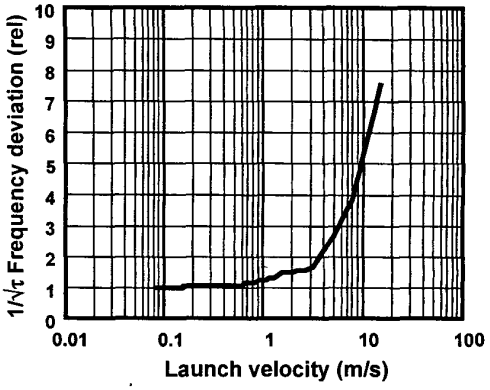

Figure 11: Composite stability of PARCS as a function of launch velocity for fixed load time (0.25 seconds). Values are relative to normal clock operations.

be traveling at nearly the same velocity, so the collision energy is reduced. Under normal operating conditions PARCS will strongly be in this latter condition, crossing into an intermediate condition at around 1 m/s, and significantly above that the thermal energy dominates. Since the variation in size is only a few percent for these fast launches, changes in the collision energy should not be a problem.

The relative phase between the cavities will be affected by changes in the temperature and microwave power incident on the mixers. We have measured the temperature dependence of a mixer to determine this sensitivity, and find that in order to maintain an uncertainty of a few parts in 10^{17} the temperature must be stable to 10 mK. The temperature need not be known accurately, but the time scale over which this temperature stability holds could well set the limit on how often we must measure the end-to-end shift.

In order to realize a factor of 100 lever on the velocity, while maintaining $\pi/2$ Rabi excitation, we require 40 dB changes in the RF power. Matched attenuators can be quite stable over such a broad range, but not at the performance level we need. A more likely approach is to maintain the power level on the mixers at the highest level, but playing one of several tricks to maintain the $\pi/2$ Rabi condition. In order to determine the power stability requirement, we have directly measured the power sensitivity of a mixer and conclude that the power must be stable to 0.1% to keep phase errors to the low 10^{-17} level. One way to realize this would be to adjust the phase of the DDS output by π on a time scale fast compared to the cavity ring time, spending a bit more time with the "plus" phase than the "minus" phase. The power in the microwave cavity will rapidly advance for a short time, then retreat, taking 100 steps forward and 99 back over and over again so that the net power in the cavity gives $\pi/2$ to the atoms. Other approaches similar in principle would involve using a variable amount of on-frequency RF with white noise added, or a mixture of on-resonant RF with an off-resonant frequency to make up the power budget without affecting the atomic spins.

One requirement of all these tricks, satisfied by the phase switching solution, is that the excitation must be spread over the entire transit time so the Rabi pedestal is not broadened artificially. This phase adjustment involves a single bit in the DDS, and seems to be the most elegant solution.

5 Acknowledgements

The authors have benefitted from discussions with the entire PARCS team. Andrea DeMarchi has previously suggested the benefits of phase modulation.

References

[1] Heavner, T.P. et al, "Characterization of a Cold Cesium Source for PARCS: Primary Atomic Reference Clock in Space", *Proc of the 2000 IEEE Freq. Control Symposium*, 2000, 656-658.

[2] Ramsey, N.F., *Molecular Beams*, Oxford at the Calrendon Press, 1956. Ch. V # 4.

[3] SenGupta, A., Popovic, D., Walls, F.L., "Cs Frequency Synthesis: A New Approach", *Proc. of the 1999 Joint Meeting of the E.F.T.F and the IEEE F.C. S*, 1999, 615.

[4] Rovera, G.D., Santarelli, G., Clairon, A., "Frequency Synthesis Chain for the Atomic Fountain Primary Standard", *IEEE Trans. Ultran., Ferroelect., Freq. Control*, **43**, 354-358 (1996).

[5] Klipstein, W., et. al. to be submitted to the *IEEE Trans. Ultras., Ferroelect., Freq. Control*

[6] Thomann, P, et.al. To be published in *Proceedings, 2001 European Frequency and Time Forum*

[7] Burt, E, et. al. To be published in *Proceedings, 2001 European Frequency and Time Forum*

[8] Vanier J., Audoin, C., *The Quantum Physics of Atomic Frequency Standards*, Adam Hilger, 1989, pg. 634.

[9] Lemonde, P., "Pharao: Etude D'une Horologe Spatiale Utilisant des Atomes Refroids Par Laser; Relisation d'un Prototype", These De Doctorate de L'Universite Paris iV, 1997.

[10] See for example the collection of articles in *IEEE Trans. Ultran., Ferroelect., Freq. Contr.*, **45**, 1998, 876-905 and the references contained therein.

[11] Kujundzic, D., Heavner, T.P., Jefferts, S.R., "Design Studies for a high-Stability Laser-Cooled Rubidium Local-Oscillator at NIST" *These Proceedings*